Inorg. Chem. **2003**, *42*, 2519–2530

Heterodimetallic Compounds Assembled from Ferrocenedicarboxylato and Ferrocenecarboxylato Ligands

Guo Dong, Li Yu-ting, Duan Chun-ying,* Mo Hong, and Meng Qing-jin*

Coordination Chemistry Institute, The State Key Laboratory of Coordination Chemistry, Nanjing University, Nanjing, 210093, P. R. China

Received August 12, 2002

Heteropolynuclear organometallic compounds have been constructed by using two kinds of ferrocene-based ligands, 1,1′-ferrocenedicarboxylic acid (H_2L^1) and ferrocenecarboxylic acid (HL^2). Reactions the ligand H_2L^1 with copper(II) and nickel(II) salts, in the presence of pyridine, give a tetranuclear Cu_2Fe_2 mixed-metallic box $Cu_2L^1{}_2(Py)_2(DMF)_2(H_2O)_2$ (**1**) and a tetranuclear heterobimetallic helix $Ni_2L^1{}_2(Py)_4(H_2O)$ (**2**), respectively. In these complexes, the ferrocene moieties show cisoid conformations which lead to the formation of the finite coordination geometry, i.e. to molecular complexes. Interactions of the ligand H_2L^1 with lanthanide ions afford two-dimensional networks $[La_2L^1{}_3(CH_3OH)_4]_\infty$ (**3**), $[Eu_2L^1{}_3(H_2O)_5]_\infty$ (**4**), and $[Gd_2L^1{}_3(CH_3OH)_2(H_2O)_3]_\infty$ (**5**), respectively, in which transoid conformations of the ferrocene moiety provide opportunities to form infinite 2-D networks. It is suggested that the conformational freedom of the ferrocene moiety makes the ligand L^1 display different conformations and coordination modes in these complexes. In addition, the $\pi\cdots\pi$ interactions related to the ferrocene moieties were also found to stabilize the supramolecular architectures in the solid state. As a comparison, reaction of lanthanide ions with the ligand HL^2 resulted in three isostructural heterodinuclear windmill-shaped compounds $Ln_2L^2{}_6(CH_3OH)_2(H_2O)_5$ [Ln = La (**6**), Eu (**7**), and Gd (**8**)] by simply diffusing the solutions of lanthanide ions into the mixture of HL^2 and NaOH, respectively. Electrochemical properties of the ferrocene-containing complexes **1**–**8** are also investigated in the solution or solid state.

Introduction

Self-organization of discrete units to form supramolecular architectures and networks of inorganic coordination compounds is a prominent field in contemporary chemistry.[1] Within this field, coordination polymers have attracted great interest with regard to their physical, electronic, catalytic, and structural properties.[2] Many topologically promising architectures have been constructed from organic multidentate ligands, such as building blocks containing nitrogen donors or polycarboxylic acids.[3,4] An assembly of metal ions and ligands in polymeric complexes can be regarded as a programmed system in which the stereo and interactive information stored in the ligands is read by the metal ions through the algorithm defined by their coordination geometry.[5] The presence of metals in different environments,

* To whom correspondence should be addressed. E-mail: duancy@nju.edu.cn (D.C.).

(1) (a) Leininger, S.; Olenyuk, B.; Stang, P. J. *Chem. Rev.* **2000**, *100*, 853. (b) Swiegers, G. F.; Malefetse, T. J. *Chem. Rev.* **2000**, *100*, 3483. (c) Moulton, B.; Zaworotko, M. J. *Chem. Rev.* **2001**, *101*, 1629. (d) Schwab, P. F. H.; Levin, M. D.; Michl, J. *Chem. Rev.* **1999**, *99*, 1863. (e) Braga, D.; Grepioni, F.; Desiraju, G. R. *Chem. Rev.* **1998**, *98*, 1375. (f) Fujita, M. *Chem. Soc. Rev.* **1998**, *27*, 417. (g) Hagrman, P. J.; Hagrman, D.; Zubieta, J. *Angew. Chem., Int. Ed.* **1999**, *38*, 2638. (h) Yaghi, O. M.; Li, H. L.; Davis, C.; Richardson, D.; Groy, T. L. *Acc. Chem. Res.* **1998**, *31*, 474.

(2) (a) Zaworotko, M. J. *Chem. Commun.* **2001**, 1. (b) O'Keeffe, M.; Eddaoudi, M.; Li, H. L.; Reineke, T.; Yaghi, O. M. *J. Solid State Chem.* **2000**, *152*, 3. (c) Kondo, M.; Yoshitomi, T.; Seki, K.; Matsuzaka, H.; Kitagawa, S. *Angew. Chem., Int. Ed. Engl.* **1997**, *36*, 1725. (d) Li, H. L.; Eddaoudi, M.; O'Keeffe, M.; Yaghi, O. M. *Nature* **1999**, *402*, 276. (e) Fujita, M.; Kwon, Y. J.; Washizu, S.; Ogura, K. *J. Am. Chem. Soc.* **1994**, *116*, 1151.

(3) (a) Seo, J. S.; Whang, D.; Lee, H.; Jun, S. I.; Oh, J.; Jeon, Y. J.; Kim, K. *Nature* **2000**, *404*, 982. (b) Chen, B. L.; Eddaoudi, M.; Hyde, S. T.; O'Keeffe, M.; Yaghi, O. M. *Science* **2001**, *291*, 1021. (c) Eddaoudi, M.; Kim, J.; Rosi, N.; Vodak, D.; Wachter, J.; O'Keefe, M.; Yaghi, O. M. *Science* **2002**, *295*, 469. (d) Chui, S. S. Y.; Lo S. M. F.; Charmant, J. P. H.; Orpen, A. G.; Williams, I. D. *Science* **1999**, *283*, 1148. (e) Withersby, M. A.; Blake, A. J.; Champness, N. R.; Cooke, P. A.; Hubberstey, P.; Schröder, M. *J. Am. Chem. Soc.* **2000**, *122*, 4044. (f) Lo, S. M. F.; Chui, S. S. Y.; Shek, L. Y.; Lin, Z. Y.; Zhan, X. X.; Wen, G. H.; Williams, I. D. *J. Am. Chem. Soc.* **2000**, *122*, 6293. (g) Manson, J. L.; Huang, Q. Z.; Lynn, J. W.; Koo, H. J.; Whangbo, M. H.; Bateman, R.; Otsuka, T.; Wada, N.; Argyriou, D. N.; Miller, J. S. *J. Am. Chem. Soc.* **2001**, *123*, 162. (h) Fletcher, A. J.; Cussen, E. J.; Prior, T. J.; Rosseinsky, M. J.; Kepert, C. J.; Thomas, K. M. *J. Am. Chem. Soc.* **2001**, *123*, 10001.

10.1021/ic0205132 CCC: $25.00
Published on Web 03/21/2003

oxidation numbers, and spin states may influence the mode of coordination of the ligand leading to a wide variety of interesting compounds. As compared to the d-block transition metals, the coordination geometry of lanthanide ions is inherently flexible and particularly attractive for the preparation of new network types, as this greater structural ambivalence will lead to the synthesis of unprecedented structures, though the high coordination numbers of lanthanide ions may cause difficulty in controlling the synthetic reactions and thereby the structures of the products.[6] Considering the difficulties inherent in the preparation of organized monometallic lanthanide complexes, it is not surprising that the selective incorporation of Ln(III) into polymetallic edifices remains a fascinating challenge in metallosupramolecular chemistry.[7]

On the other hand, from the viewpoint of constructing functional supramolecular compounds, it may be interesting to incorporate functional groups on the ligand instead of such nonfunctional spacers.[8] Among them, redox-active coordination polymers are of great interest because redox functions may lead to a variety of intriguing electrical, photophysical, or catalytic phenomena.[9] Organometallic compounds, especially ferrocene and its derivatives, have been pursed with the objective of generating materials possessing useful electrochemical, magnetic, and optical and nonlinear optical properties.[10] And these include redox-active materials for modification of electrodes or materials, which can function as miltielectron redox systems or biosensors.[11] In addition, the conformational freedom of ferrocene and a large number of polarized C−H systems making C−H···π weak interactions important in crystal packing afford opportunities for generating novel topologies.[12,13] Here we use ferrocene-containing ligand 1,1′-ferrocenedicarboxylic acid (H_2L^1) to construct ferrocene-containing heterobimetallic coordination polymers. It is suggested that introducing a ferrocene group into coordination polymer systems not only incorporates a redox-active group but also leads to interesting assembled structures because of the conformational flexibility of the ferrocene moieties and the varying coordination numbers of metal ions. Although carboxylate ligands are known to bridge metal centers and are potential candidates for the formation of extended arrays, carboxylic acids based on ferrocene moieties are not well studied. Especially, lanthanide−ferrocene coordination polymers have not been reported in the literature to our best knowledge. In this paper, we report the structures and electrochemical properties of two new d-block transition metal ferrocene-containing complexes

(4) (a) Noro, S.; Kitaura, R.; Kondo, M.; Kitagawa, S.; Ishii, T.; Matsuzaka, H.; Yamashita, M. *J. Am. Chem. Soc*. **2002**, *124*, 2568. (b) Noveron, J. C.; Lah, M. S.; Del Sesto, R. E.; Arif, A. M.; Miller, J. S.; Stang, P. J. *J. Am. Chem. Soc*. **2002**, *124*, 6613. (c) Cui, Y.; Evans, O. R.; Ngo, H. L.; White, P. S.; Lin, W. B. *Angew. Chem., Int. Ed*. **2002**, *41*, 1159. (d) Pschirer, N. G.; Ciurtin, D. M.; Smith, M. D.; Bunz, U. H. F.; zur Loye, H. C. *Angew. Chem., Int. Ed*. **2002**, *41*, 583. (e) Kitaura, R.; Fujimoto, K.; Noro, S.; Kondo, M.; Kitagawa, S. *Angew. Chem., Int. Ed*. **2002**, *41*, 133. (f) Xiong, R. G.; You, X. Z.; Abrahams, B. F.; Xue, Z. L.; Che, C. M. *Angew. Chem., Int. Ed*. **2001**, *40*, 4422. (g) Boldog, I.; Rusanov, E. B.; Chernega, A. N.; Sieler, J.; Domasevitch, K. V. *Angew. Chem., Int. Ed*. **2001**, *40*, 3435. (h) Ma, B. Q.; Gao, S.; Su, G.; Xu, G. X. *Angew. Chem., Int. Ed*. **2001**, *40*, 434. (i) Biradha, K.; Hongo, Y.; Fujita, M. *Angew. Chem., Int. Ed*. **2000**, *39*, 3843. (j) Carlucci, L.; Ciani, G.; Moret, M.; Proserpio, D. M.; Rizzato, S. *Angew. Chem., Int. Ed*. **2000**, *39*, 1506. (k) Noro, S.; Kitagawa, S.; Kondo, M.; Seki, K. *Angew. Chem., Int. Ed*. **2000**, *39*, 2082. (l) Horikoshi, R.; Mochida, T.; Moriyama, H. *Inorg. Chem*. **2002**, *41*, 3017.

(5) Lehn, J. M. *Supramolecular Chemistry-Concepts and Perspectives*; VCH: Weinheim, Germany, 1995.

(6) (a) Long, D. L.; Blake, A. J.; Champness, N. R.; Schröder, M. *Chem. Commun*. **2000**, 1369. (b) Goodgame, D. M. L.; Menzer, S.; Ross, A. T.; Williams, D. J. *J. Chem. Soc., Chem. Commun*. **1994**, 2605. (c) Goodgame, D. M. L.; Menzer, S.; Smith, A. M.; Williams, D. J. *Chem. Commun*. **1997**, 339. (d) Reineke, T. M.; Eddaoudi, M.; Fehr, M.; Kelley, D.; Yaghi, O. M. *J. Am. Chem. Soc*. **1999**, *121*, 1651. (e) Reineke, T. M.; Eddaoudi, M.; O'Keeffe, M.; Yaghi, O. M. *Angew. Chem., Int. Ed*. **1999**, *38*, 2590. (f) Liang, Y. C.; Cao, R.; Su, W. P.; Hong, M. C.; Zhang, W. J. *Angew. Chem., Int. Ed*. **2000**, *39*, 3304. (g) Mortl, K. P.; Sutter, J. P.; Golhen, S.; Ouahab, L.; Kahn, O. *Inorg. Chem*. **2000**, *39*, 1626. (h) Pan, L.; Huang, X. Y.; Li, J.; Wu, Y. G.; Zheng, N. W. *Angew. Chem., Int. Ed*. **2000**, *39*, 527. (i) Cao, R.; Sun, D. F.; Liang, Y. C.; Hong, M. C.; Tatsumi, K.; Shi, Q. *Inorg. Chem*. **2002**, *41*, 2087.

(7) Bünzli, J.-C. G.; Piguet, C. *Chem. Rev*. **2002**, *102*, 1897.

(8) (a) Fujita, N.; Biradha, K.; Fujita, M.; Sakamoto, S.; Yamaguchi, K. *Angew. Chem., Int. Ed*. **2001**, *40*, 1718. (b) Abrahams, B. F.; Hoskins, B. F.; Michail, D. M.; Robson, R. *Nature* **1994**, *369*, 727. (c) Lin, K. J. *Angew. Chem., Int. Ed*. **1999**, *38*, 2730. (d) Sharma, C. V. K.; Broker, G. A.; Huddleston, J. G.; Baldwin, J. W.; Metzger, R. M.; Rogers, R. D. *J. Am. Chem. Soc*. **1999**, *121*, 1137.

(9) (a) Audrieux, C. P.; Blocman, C.; Dumas-Bouchiat, J. M.; M'Halla, F.; Savéant, J. M. *J. Am. Chem. Soc*. **1980**, *102*, 3806. (b) Audrieux, C. P.; Haas, O.; Savéant, J. M. *J. Am. Chem. Soc*. **1986**, *108*, 8175. (c) Balzani, V.; Juris, A.; Venturi, M.; Campagna, S.; Serroni, S. *Chem. Rev*. **1996**, *96*, 759. (d) Chandrasekhar, V.; Nagendran, S.; Bansal, S.; Kozee, M. A.; Powell, D. R. *Angew. Chem., Int. Ed*. **2000**, *39*, 1833. (e) Cotton, F. A.; Daniels, L. M.; Lin, C.; Murillo, C. A. *J. Am. Chem. Soc*. **1999**, *121*, 4538. (f) Pal, I.; Basuli, F.; Mak, T. C. W.; Bhattacharya, S. *Angew. Chem., Int. Ed*. **2001**, *40*, 2923. (g) Carlucci, L.; Ciani, G.; Porta, F.; Proserpio, D. M.; Santagostini, L. *Angew. Chem., Int. Ed*. **2002**, *41*, 1907. (h) Steed, J. W.; Atwood, J. L. *Supramolecular Chemistry*; Wiley & Sons: Chichester, U.K., 2000.

(10) (a) Plenio, H.; Aberle, C.; Al Shihadeh, Y.; Lloris, J. M.; Martinez-Manez, R.; Pardo, T.; Soto, J. *Chem.—Eur. J*. **2001**, *7*, 2848. (b) Jutzi, P.; Lenze, N.; Neumann, B.; Stammler, H. G. *Angew. Chem., Int. Ed*. **2001**, *40*, 1424. (c) Miller, J. S.; Epstein, A. J.; Reiff, W. M. *Acc. Chem. Res*. **1988**, *21*, 114. (d) *Ferrocenes: Homogeneous Catalysis, Organic Synthesis, Materials Science*; Togni, A., Hayashi, T., Eds.; VCH: Weinheim, Germany, 1995. (e) Long, N. J. *Metallocenes: An Introduction to Sandwich Complexes*; Blackwell Science, Inc.: Cambridge, MA, 1998. (f) Bradley, S.; Camm, K. D.; Liu, X. M.; McGowan, P. C.; Mumtaz, R.; Oughton, K. A.; Podesta, T. J.; Thornton-Pett, M. *Inorg. Chem*. **2002**, *41*, 715.

(11) (a) Evans, D. H.; Lehmann, M. W. *Acta Chem. Scand*. **1999**, *53*, 765. (b) Barrière, F.; Camire, N.; Geiger, W. E.; Mueller-Westerhoff, U. T.; Sanders, R. *J. Am. Chem. Soc*. **2002**, *124*, 7262. (c) Demadis, K. D.; Hartshorn, C. M.; Meyer, T. J. *Chem. Rev*. **2001**, *101*, 2655. (d) Flanagan, J. B.; Margel, S.; Bard, A. J.; Anson, F. C. *J. Am. Chem. Soc*. **1978**, *100*, 4248. (e) Astruc, D. *Top. Curr. Chem*. **1991**, *160*, 47. (f) Degani, Y.; Heller, A. *J. Phys. Chem*. **1987**, *91*, 1285.

(12) (a) Braga, D.; Maini, L.; Grepioni, F. *J. Organomet. Chem*. **2000**, *594*, 101. (b) Crespo, O.; Gimeno, M. C.; Jones, P. G.; Laguna, A.; Sarroca, C. *Chem. Commun*. **1998**, 1481. (c) Crespo, O.; Canales, F.; Gimeno, M. C.; Jones, P. G.; Laguna, A. *Organometallics* **1999**, *18*, 3142. (d) Grosche, M.; Herdtweck, E.; Peters, F.; Wagner, M. *Organometallics* **1999**, *18*, 4669. (e) Maricic, S.; Berg, U.; Frejd, T. *Tetrahedron* **2002**, *58*, 3085. (f) Shum, S. P.; Pastor, S. D.; Rihs, G. *Inorg. Chem*. **2002**, *41*, 127. (g) Mata, J. A.; Peris, E. *J. Chem. Soc., Dalton Trans*. **2001**, 3634. (h) Moriuchi, T.; Yoshida, K.; Hirao, T. *Organometallics* **2001**, *20*, 3101. (i) Moriuchi, T.; Nomoto, A.; Yoshida, K.; Ogawa, A.; Hirao, T. *J. Am. Chem. Soc*. **2001**, *123*, 68. (j) Braga, D.; Polito, M.; Bracaccini, M.; D'Addario, D.; Tagliavini, E.; Proserpio, D. M.; Grepioni, F. *Chem. Commun*. **2002**, 1080.

(13) (a) Fang, C. J.; Duan, C. Y.; He, C.; Han, G.; Meng, Q. J. *New J. Chem*. **2000**, *24*, 697. (b) Fang, C. J.; Duan, C. Y.; Mo, H.; He, C.; Meng, Q. J.; Liu, Y. J.; Mei, Y. H.; Wang, Z. M. *Organometallics* **2001**, *20*, 2525. (c) Fang, C. J.; Duan, C. Y.; He, C.; Meng, Q. J. *Chem. Commun*. **2000**, 1187. (d) Fang, C. J.; Duan, C. Y.; Guo, D.; He, C.; Meng, Q. J.; Wang, Z. M.; Yan, C. H. *Chem. Commun*. **2001**, 2540. (e) Guo, D.; Han, G.; Duan, C. Y.; Pang, K. L.; Meng, Q. J. *Chem. Commun*. **2002**, 1096. (f) Guo, D.; Mo, H.; Duan, C. Y.; Lu, F.; Meng, Q. J. *J. Chem. Soc., Dalton Trans*. **2002**, 2593.

$Cu_2L^1{}_2(Py)_2(DMF)_2(H_2O)_2$ (**1**) and $Ni_2L^1{}_2(Py)_4(H_2O)$ (**2**), as well as three lanthanide-ferrocene 2-D coordination polymers $[La_2L^1{}_3(CH_3OH)_4]_\infty$ (**3**), $[Eu_2L^1{}_3(H_2O)_5]_\infty$ (**4**), and $[Gd_2L^1{}_3(CH_3OH)_2(H_2O)_3]_\infty$ (**5**). And as a comparison, lanthanide−ferrocene complexes based on ferrocenecarboxylic acid (HL^2), $Ln_2L^2{}_6(CH_3OH)_2(H_2O)_5$ [Ln = La (**6**), Eu (**7**), and Gd (**8**)], were also synthesized and characterized.

Experimental Section

Materials and Analyses. All chemicals were of reagent grade quality obtained from commercial sources and used without further purification except for 1,1′-ferrocenedicarboxylic acid[14] and ferrocenecarboxylic acid,[15] which were synthesized by following the literature procedures. Elemental analyses (C, H, and N) were carried out on a Perkin-Elmer 240 analyzer. IR spectra were recorded on a Vector 22 Bruker spectrophotometer with KBr pellets in the 4000−400 cm^{-1} regions. UV/vis spectra were obtained at room temperature on a Shimmadzu 3100 spectrophotometer in DMF. Cyclic voltammograms and differential pulse voltammetry results were recorded with an EG & G PAR model 273 instrument. The solution-state measurements were performed in DMF with *n*-Bu_4NClO_4 (0.1 mol·dm^{-3}) as supporting electrolyte, in a three-electrode cell with a pure Ar gas inlet and outlet, which has a 50 ms pulse width with current samples 40 ms after the pulse was applied. A sweep rate of 20 mV s^{-1} was used in all pulse experiments. The cell comprises a platinum wire working electrode, a platinum auxiliary electrode, and an Ag/AgCl wire reference electrode. Ferrocene (1.0×10^{-3} mol dm^{-3}) was used as external standard. The solid-state voltammograms[16] were measured by using a carbon-paste working electrode; well-ground mixtures of each bulk sample and carbon paste (graphite and mineral oil) were set in the channel of a glass tube and connected to a copper wire. A platinum-wire counter electrode and an Ag/AgCl reference electrode were used. Measurements were performed by using a three-electrode system in 0.1 mol dm^{-3} $NaClO_4$ aqueous solutions at a scan rate of 20 mV s^{-1}, in the range 0−1.0 V. The ferrocene in the solid state was also used as external standard with $E_{1/2} = 0.25$ V vs the Ag/AgCl electrode.

Caution! *Although no problems were encountered in this work, the salt perchlorates are potentially explosive. They should be prepared in small quantities and handled with care.*

$Cu_2L^1{}_2(Py)_2(DMF)_2(H_2O)_2$ (1). A DMF mixture (5 mL) of $Cu(BF_4)_2$ (0.07 g, 0.30 mmol) and 1,1′-ferrocenedicarboxylic acid (0.08 g, 0.30 mmol) was added into a small tube, which was placed in a larger vial containing pyridine (10 mL). The larger vial was sealed and left undisturbed in darkness at room temperature for 15 days. The green block crystals on the bottom of the vial were isolated and then washed with 3 × 10 mL of ethanol to give 0.11 g (73%) of product. Anal. Calcd for $C_{40}H_{44}N_4Fe_2Cu_2O_{12}$, **1**: C, 47.5; H, 4.4; N, 5.5. Found: C, 47.7; H, 3.9; N, 5.2. IR (KBr, cm^{-1}): 3425 m, 1606 s, 1578 vs, 1474 s, 1449 s, 1390 s, 1353 s, 1335 m, 1182 w, 1023 w, 799 m, 761 m, 689 m, 517 w. UV/vis [DMF; λ_{max}/nm (ϵ/dm^3 mol^{-1} cm^{-1})]: 304 (20 250), 373 (11 250), 814 (3750).

$Ni_2L^1{}_2(Py)_4(H_2O)$ (2). The procedure was similar to that described for the preparation of **1**, except that $Ni(BF_4)_2$ (0.07 g, 0.30 mmol) was used instead of $Cu(BF_4)_2$. The product, **2**, was obtained in 65% yield. Anal. Calcd for $C_{44}H_{38}N_4Fe_2Ni_2O_9$, **2**: C, 53.1; H, 3.9; N, 5.6. Found: C, 53.5; H, 3.9; N, 5.4. IR (KBr, cm^{-1}): 3426 w, 1656 m, 1602 s, 1484 s, 1449 s, 1393 s, 1361 s, 1219 w, 1040 m, 759 m, 700 m, 514 m. UV/vis [DMF; λ_{max}/nm (ϵ/dm^3 mol^{-1} cm^{-1})]: 301 (24 000), 435 (12 300).

$[La_2L^1{}_3(CH_3OH)_4]_\infty$ (3). A solution of 1,1′-ferrocenedicarboxylic acid (0.08 g, 0.30 mmol) and NaOH (0.02 g, 0.62 mmol) in methanol (10 mL) was layered onto a solution of $La(NO_3)_3$ (0.07 g, 0.20 mmol) in water (10 mL). The solutions were left for 1 month at room temperature in darkness to afford red block crystals (0.07 g, 0.06 mmol) suitable for X-ray work in a modest yield (60%). Anal. Calcd for $C_{40}H_{40}Fe_3La_2O_{16}$, **3**: C, 39.3; H, 3.3. Found: C, 39.4; H, 3.5. IR (KBr, cm^{-1}): 3418 m, 3141 m, 2938 w, 1580 m, 1530 s, 1492 s, 1471 s, 1396 s, 1349 m, 1189 m, 1025 m, 803 m, 608 w, 561 w, 515 m.

$[Eu_2L^1{}_3(H_2O)_5]_\infty$ (4). The way was similar to that described for the preparation of **3**, except that $EuCl_3$ (0.05 g, 0.20 mmol) was used instead of $La(NO_3)_3$. The product, **4**, was obtained in 71% yield. Anal. Calcd for $C_{36}H_{34}Fe_3Eu_2O_{17}$, **4**: C, 35.7; H, 2.8. Found: C, 35.8; H, 3.2. IR (KBr, cm^{-1}): 3321 s, 1525 s, 1483 s, 1395 s, 1354 m, 1190 w, 1029 w, 822 m, 795 m, 676 w, 548 w, 502 m.

$[Gd_2L^1{}_3(CH_3OH)_2(H_2O)_3]_\infty$ (5). The way was similar to that described for the preparation of **3**, except that $GdCl_3$ (0.05 g, 0.20 mmol) was used instead of $La(NO_3)_3$. The product, **5**, was obtained in 47% yield. Anal. Calcd for $C_{38}H_{38}Fe_3Gd_2O_{17}$, **5**: C, 36.6; H, 3.1. Found: C, 36.3; H, 3.0. IR (KBr, cm^{-1}): 3386 m, 1529 vs, 1484 vs, 1394 vs, 1356 s, 1190 m, 1031 w, 802 m, 508 m.

$La_2L^2{}_6(CH_3OH)_2(H_2O)_5$ (6). A solution of ferrocenecarboxylic acid (0.14 g, 0.60 mmol) and NaOH (0.02 g, 0.60 mmol) in methanol (10 mL) was layered onto a solution of $La(NO_3)_3$ (0.07 g, 0.20 mmol) in water (10 mL). The solutions were left for 1 month at room temperature in darkness to afford red block crystals (0.13 g, 0.07 mmol) suitable for X-ray work in a good yield (70%). Anal. Calcd for $C_{68}H_{72}Fe_6La_2O_{19}$, **6**: C, 45.2; H, 4.0. Found: C, 45.1; H, 3.6. IR (KBr, cm^{-1}): 3406 w, 1524 s, 1477 vs, 1392 vs, 1360 s, 1189 w, 1026 w, 816 m, 507 m. UV/vis [DMF; λ_{max}/nm (ϵ/dm^3 mol^{-1} cm^{-1})]: 297 (18 000), 340 (6700), 450 (3600).

$Eu_2L^2{}_6(CH_3OH)_2(H_2O)_5$ (7). The way was similar to that described for the preparation of **6**, except that $EuCl_3$ (0.05 g, 0.20 mmol) was used instead of $La(NO_3)_3$. The product, **7**, was obtained in 58% yield. Anal. Calcd for $C_{68}H_{72}Fe_6Eu_2O_{19}$, **7**: C, 44.6; H, 4.0. Found: C, 44.4; H, 3.9. IR (KBr, cm^{-1}): 3422 w, 1522 vs, 1468 vs, 1391 vs, 1360 s, 1188 w, 1025 w, 815 m, 555 w, 507 m. UV/vis [DMF; λ_{max}/nm (ϵ/dm^3 mol^{-1} cm^{-1})]: 310 (19 200), 337 (6100), 441 (4500).

$Gd_2L^2{}_6(CH_3OH)_2(H_2O)_5$ (8). The way was similar to that described for the preparation of **6**, except that $GdCl_3$ (0.05 g, 0.20 mmol) was used instead of $La(NO_3)_3$. The product, **8**, was obtained in 64% yield. Anal. Calcd for $C_{68}H_{72}Fe_6Gd_2O_{19}$, **8**: C, 44.3; H, 3.9. Found: C, 44.1; H, 4.0. IR (KBr, cm^{-1}): 3421 w, 1523 vs, 1466 vs, 1388 vs, 1359 s, 1186 w, 1106 w, 1002 w, 810 m, 506 m. UV/vis [DMF; λ_{max}/nm (ϵ/dm^3 mol^{-1} cm^{-1})]: 299 (19 400), 342 (6400), 454 (3300).

Crystallographic Analyses. Parameters for data collection and refinement of complexes **1**−**8** are summarized in Tables 1−3. The intensities of complexes **1** and **2** were collected on an Enraf-Nonius CCD system[17] with graphite-monochromated Mo Kα radiation (λ = 0.710 73 Å). Data were reduced using the HKL Denzo and

(14) Rausch, M. D.; Ciappenelli, D. J. *J. Organomet. Chem*. **1967**, *10*, 127.
(15) Rinehart, K. L., Jr.; Curby, R. J., Jr.; Sokol, P. E. *J. Am. Chem. Soc*. **1957**, *79*, 3420.
(16) (a) Noro, S.; Kondo, M.; Ishii, T.; Kitagawa, S.; Matsuzaka, H. *J. Chem. Soc., Dalton Trans*. **1999**, 1569. (b) Kondo, M.; Shimamura, M.; Noro, S.; Kimura, Y.; Uemura, K.; Kitagawa, S. *J. Solid State Chem*. **2000**, *152*, 113.
(17) *"Collect" data collection software*; Nonius BV.: Delft, The Netherlands, 1998.

Table 1. Crystallographic Data for Complexes **1** and **2**

	1	**2**
formula	$C_{40}H_{44}Cu_2Fe_2N_4O_{12}$	$C_{44}H_{38}Fe_2N_4Ni_2O_9$
fw	1011.57	995.90
T/°C	293(2)	293(2)
cryst syst	monoclinic	orthorhombic
space group	$P2_1/c$	Pbcn
a/Å	11.480(2)	19.047(4)
b/Å	18.910(4)	15.460(3)
c/Å	9.654(2)	13.989(3)
β/deg	108.47(3)	
V/Å^3	1987.7(7)	4119.3(14)
Z	2	4
ρ_{calcd}/g cm^{-3}	1.690	1.606
μ/cm^{-1}	1.841	1.653
R_1[a]	0.0497	0.0412
wR_2[a]	0.0815	0.0785

[a] $R_1 = \sum||F_o| - |F_c||/\sum|F_o|$; $wR_2 = [\sum w(F_o^2 - F_c^2)^2/\sum w(F_o^2)^2]^{1/2}$.

Table 2. Crystallographic Data for Complexes **3**−**5**

	3	**4**	**5**
formula	$C_{40}H_{40}Fe_3La_2O_{16}$	$C_{36}H_{34}Eu_2Fe_3O_{17}$	$C_{38}H_{38}Fe_3Gd_2O_{17}$
fw	1222.09	1210.10	1248.73
T/°C	293(2)	293(2)	293(2)
cryst syst	triclinic	monoclinic	monoclinic
space group	$P\bar{1}$	$P2/n$	$P2/n$
a/Å	9.515(1)	11.219(2)	11.259(1)
b/Å	10.332(2)	10.270(3)	10.263(1)
c/Å	11.094(2)	17.088(6)	17.231(2)
α/deg	92.139(3)		
β/deg	109.367(3)	91.46(3)	91.905(2)
γ/deg	97.289(2)		
V/Å^3	1016.9(3)	1968.2(10)	1989.9(4)
Z	1	2	2
ρ_{calcd}/g cm^{-3}	1.996	2.042	2.084
μ/cm^{-1}	3.174	4.294	4.431
R_1[a]	0.0430	0.0732	0.0448
wR_2[a]	0.0673	0.1829	0.1161

[a] $R_1 = \sum||F_o| - |F_c||/\sum|F_o|$; $wR_2 = [\sum w(F_o^2 - F_c^2)^2/\sum w(F_o^2)^2]^{1/2}$.

Table 3. Crystallographic Data for Complexes **6**−**8**

	6	**7**	**8**
formula	$C_{68}H_{72}Fe_6La_2O_{19}$	$C_{68}H_{72}Fe_6Eu_2O_{19}$	$C_{68}H_{72}Fe_6Gd_2O_{19}$
fw	1806.18	1832.28	1842.86
T/°C	293(2)	293(2)	293(2)
cryst syst	triclinic	triclinic	triclinic
space group	$P\bar{1}$	$P\bar{1}$	$P\bar{1}$
a/Å	8.879(1)	8.798(1)	8.777(1)
b/Å	14.454(2)	14.445(1)	14.440(1)
c/Å	15.298(2)	15.254(2)	15.220(1)
α/deg	117.445(3)	117.229(1)	117.255(1)
β/deg	105.601(2)	105.301(2)	105.20(2)
γ/deg	90.953(2)	91.031(2)	91.015(2)
V/Å^3	1655.2(4)	1640.7(3)	1633.3(3)
Z	1	1	1
ρ_{calcd}/g cm^{-3}	1.812	1.854	1.874
μ/cm^{-1}	2.609	3.242	3.367
R_1[a]	0.0384	0.0323	0.0291
wR_2[a]	0.0586	0.0607	0.0654

[a] $R_1 = \sum||F_o| - |F_c||/\sum|F_o|$; $wR_2 = [\sum w(F_o^2 - F_c^2)^2/\sum w(F_o^2)^2]^{1/2}$.

MaXus program,[18] and a semiempirical absorption correction from a ψ-scan was applied.[19] Intensities of the complex **4** were collected on a Siemens P4 four-circle diffractometer with graphite-monochromatic Mo Kα radiation ($\lambda = 0.710\ 73$ Å) using the $\omega-2\theta$ scan mode. Data were corrected for Lorenz−polarization effects during data reduction using XSCANS,[20] and a semiempirical absorption correction from ψ-scans was applied. Intensities of complexes **3** and **5**−**8** were collected on a Siemens SMART-CCD diffractometer with graphite-monochromatic Mo Kα radiation ($\lambda = 0.710\ 73$ Å) using the SMART and SAINT[21] programs. The structures were solved by direct methods and refined on F^2 using full-matrix least-squares methods with SHELXTL version 5.1.[22] Anisotropic thermal parameters were refined for the non-hydrogen atoms. Hydrogen atoms were localized in their calculation positions and refined using a riding model.

Results and Discussion

Syntheses. The study of heteropolynuclear organometallic compounds has attracted great interest in the past decade. One of the methods used to prepare heteropolymetallic compounds is based on the choice of ferrocenyl substrates containing heteroatoms (mainly nitrogen, sulfur, phosphorus, or oxygen) and/or unsaturated groups with good donor abilities, which may allow the coordination of one or more metal ions.[23] The synthesis and characterization of transition metal complexes containing 1,1′-ferrocenedicarboxylato(2−) or ferrocenecarboxylato(1−) ligand appear to be especially interesting, since depending on the mode of coordination of this group to one or more metal cations, it may lead to a wide variety of interesting compounds.[9e,24] In the previous work, compounds usually have been obtained by reacting the metal ions with ligands in certain solvents and evaporating the resulting solution. Herein, we prepared present compounds by simply diffusing a pyridine solution into a mixture of the metal ion and the ligand or directly diffusing a solution of the metal ion into the solution of carboxylic acid in the presence of NaOH. Owing to the tendency for high coordination, lanthanide ions favor the formation of

(18) (a) Otwinowski, Z.; Minor, W. *Processing of X-ray Diffraction Data Collected in Oscillation Mode*; Methods in Enzymology, Vol. 276: Macromolecular Crystallography; Carter, C. W., Jr., Sweet, R. M., Eds.; Academic Press: New York, 1997; Part A, pp 307−326. (b) Mackay, S.; Gilmore, C. J.; Tremayne, M.; Stuart, N,; Shankland, K. *maXus: a computer program for the solution and refinement of crystal structures from diffraction data*; University of Glasgow, Glasgow, Scotland, U.K., Nonius BV, Delft, The Netherlands, and MacScience Co. Ltd., Yokohama, Japan, 1998.

(19) (a) Blessing, R. H. *Acta Crystallogr.* **1995**, *A51*, 33. (b) Blessing, R. H. *J. Appl. Crystallogr.* **1997**, *30*, 421.

(20) *XSCANS*, version 2.1; Siemens Analytical X-ray Instruments, Inc.: Madison, WI, 1994.

(21) *SMART and SAINT, Area Detector Control and Integration Software*; Siemens Analytical X-ray Systems, Inc.: Madison, WI, 1996.

(22) Sheldrick, G. M. *SHELXTL V5.1, Software Reference Manual*; Bruker AXS, Inc.: Madison, WI, 1997.

(23) (a) Togni, A.; Haltermann, R. L. In *Metallocenes*; Wiley-VCH: Weinheim, Germany, 1998. (b) Whittall, I. R.; McDonagh, A. M.; Humphrey, M. G.; Samoc, M. *Adv. Organomet. Chem.* **1998**, *42*, 291. (c) Severin, K.; Bergs, R.; Beck, W. *Angew. Chem., Int. Ed.* **1998**, *37*, 1635. (d) Zhuravel, M. A.; Glueck, D. S.; Liable-Sands, L. M.; Rheingold, A. L. *Organometallics* **1998**, *17*, 574. (e) Gibson, V. C.; Long, N. J.; White, A. J. P.; Williams, C. K.; Williams, D. J. *Organometallics* **2000**, *19*, 4425. (f) Gibson, V. C.; Long, N. J.; White, A. J. P.; Williams, C. K.; Williams, D. J. *Chem. Commun.* **2000**, 2359.

(24) (a) Abuhijleh, A. L.; Woods, C. *J. Chem. Soc., Dalton Trans.* **1992**, 1249. (b) Churchill, M. R.; Li, Y. J.; Nalewajek, D.; Schaber, P. M.; Dorfman, J. *Inorg. Chem.* **1985**, *24*, 2684. (c) Costa, R.; López, C.; Molins, E.; Espinosa, E. *Inorg. Chem.* **1998**, *37*, 5686. (d) López, C.; Costa, R.; Illas, F.; Molins, E.; Espinosa, E. *Inorg. Chem.* **2000**, *39*, 4560. (e) Costa, R.; López, C.; Molins, E.; Espinosa, E.; Pérez, J. *J. Chem. Soc., Dalton Trans.* **2001**, 2833. (f) Christie, S. D.; Subramanian, S.; Thompson, L. K.; Zaworotko, M. J. *J. Chem. Soc., Chem. Commun.* **1994**, 2563. (g) Chandrasekhar, V.; Nagendran, S.; Bansal, S.; Kozee, M. A.; Powell, D. R. *Angew. Chem., Int. Ed.* **2000**, *39*, 1833.

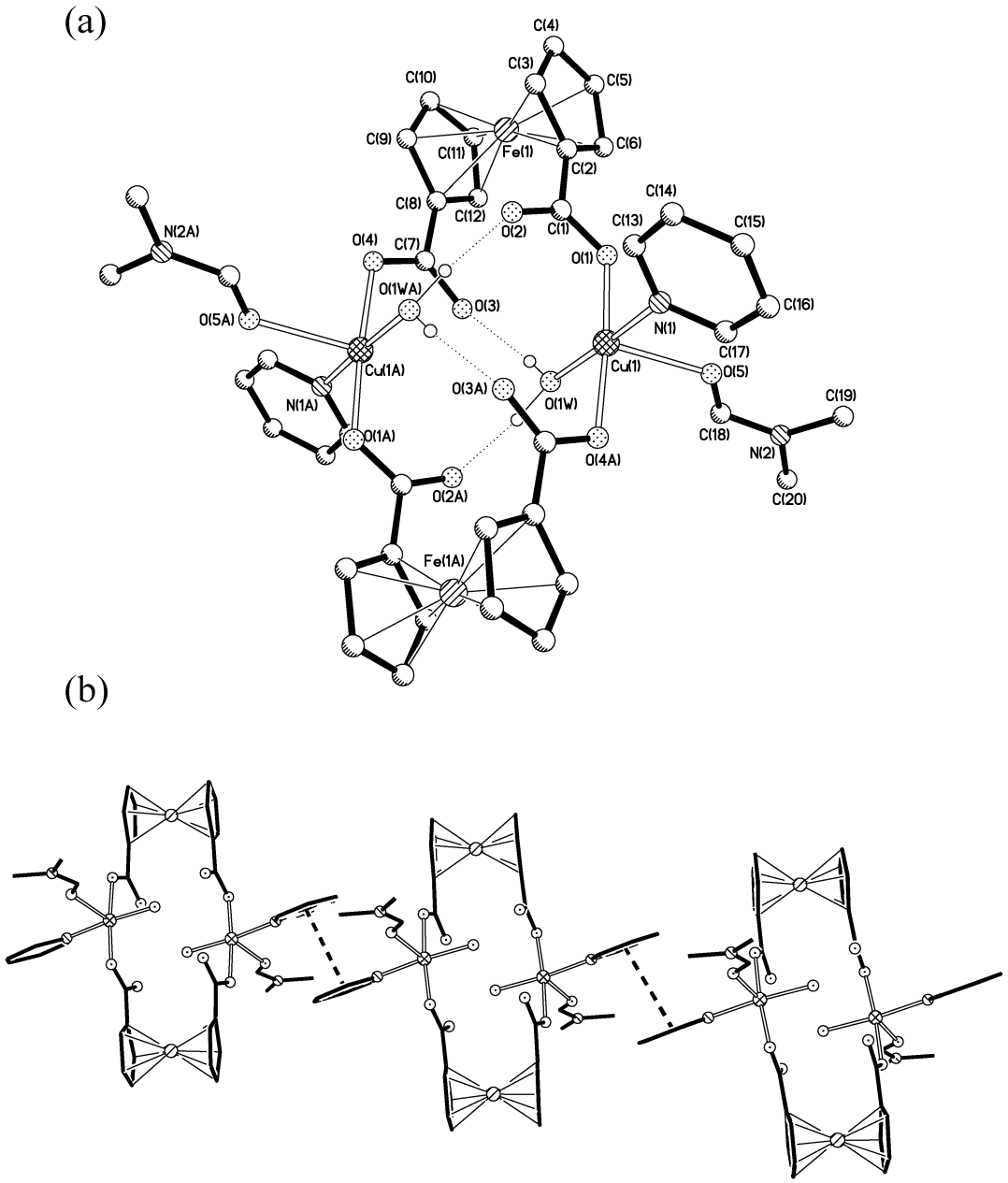

Figure 1. (a) Molecular structure of **1** with the atom numbering scheme. Hydrogen atoms apart from those on water molecules are omitted for clarity. (b) View of one-dimensional chain in complex **1** showing the intermolecular $\pi-\pi$ stacking interactions.

condensed structures;[25] however, by liberation of some small ligands bonded to lanthanides ions, such as water, these structures can be transferred to less condensed frameworks.

$Cu_2L^1_2(Py)_2(DMF)_2(H_2O)_2$ (1). Compound **1** displays a centrosymmetric bimetallic molecular box (Figure 1a) constituted by the linkage of two $Cu(L^1)(Py)(DMF)(H_2O)$ units. The four coplanar metals form a slightly distorted rhombus with the sides of 5.69 and 5.73 Å and the interior angles of 50 and 130°, respectively. The separation between the two Cu(II) ions is 4.85 Å. The carboxyl groups of 1,1′-ferrocenedicarboxylic acid are deprotonated, in agreement with the IR data in which no strong absorption peaks around 1700 cm^{-1} for COOH are observed. The so-formed macrocycle presents two bridging *O*,*O*′-ferrocenedicarboxylato moieties with the monodentate *syn*-coordination of the carboxy groups. The overall conformation of the ferrocenedicarboxylato moietiy can be regarded as a synperiplanar conformation (Chart 1) with the torsion angle for these moieties being ca. 0.1° in respect to the usual definition used with [1,1′]-ferrocenophanes.[26] This conformation is different from the synclinal (staggered) conformation (Chart 1) of the ferrocene group in bimetallic macrocycle compound [Zn-

(25) (a) Wu, L. P.; Munakata, M.; Kuroda-Sowa, T.; Maekawa, M.; Suenaga, Y. *Inorg. Chim. Acta* **1996**, *249*, 183. (b) Seddon, J. A.; Jackson, A. R. W.; Kresinski, R. A.; Platt, A. W. G. *Polyhedron* **1996**, *15*, 1899.

(26) (a) Löwendahl, J. M.; Håkansson, M. *Organometallics* **1995**, *14*, 4736. (b) Mueller-Westerhoff, U. T.; Swiegers, G. F.; Haas, T. J. *Organometallics* **1992**, *11*, 3411. (c) Mai, J. F.; Yamamoto, Y. *J. Organomet. Chem*. **1998**, *560*, 223.

Chart 1. Conformations of the Ferrocenyl Rings: (a) Synperiplanar; (b) Synclinal (Staggered); (c) Synclinal (Eclipsed); (d) Anticlinal (Staggered); (e) Anticlinal (Eclipsed); (f) Antiperiplanar

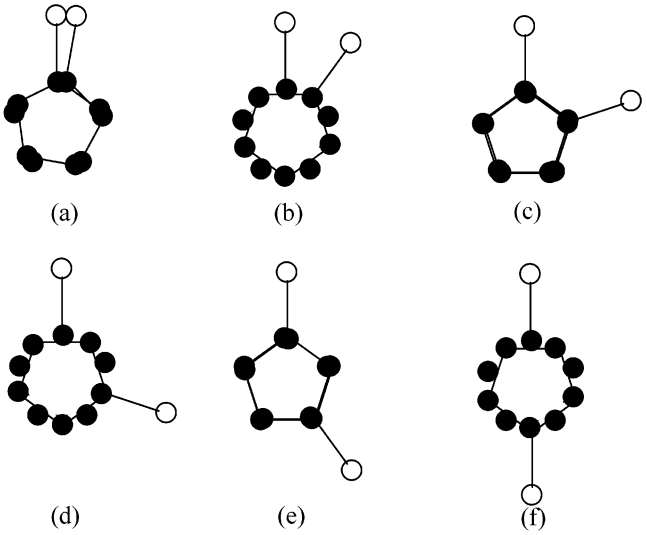

Table 4. Selected Bond Lengths (Å) and Bond Angles (deg) of Compounds **1** and **2** with Estimated Standard Deviations in Parentheses

1[a]

Cu(1)−O(1)	1.949(3)	Cu(1)−O(4A)	1.966(3)
Cu(1)−O(1W)	1.986(3)	Cu(1)−N(1)	2.035(4)
Cu(1)−O(5)	2.297(3)		
O(1)−Cu(1)−O(4A)	175.0(1)	O(1)−Cu(1)−O(1W)	88.8(1)
O(4A)−Cu(1)−O(1W)	86.6(1)	O(1)−Cu(1)−N(1)	93.7(1)
O(4A)−Cu(1)−N(1)	90.8(1)	O(1W)−Cu(1)−N(1)	174.7(1)
O(1)−Cu(1)−O(5)	91.8(1)	O(4A)−Cu(1)−O(5)	90.7(1)
O(1W)−Cu(1)−O(5)	95.7(1)	N(1)−Cu(1)−O(5)	89.0(1)

2[b]

Ni(1)−O(1)	1.992(2)	Ni(1)−O(3A)	2.073(2)
Ni(1)−N(2)	2.078(3)	Ni(1)−O(2A)	2.088(2)
Ni(1)−N(1)	2.119(3)	Ni(1)−O(1W)	2.147(2)
O(1)−Ni(1)−O(3A)	177.6(1)	O(1)−Ni(1)−N(2)	89.0(1)
O(3A)−Ni(1)−N(2)	91.9(1)	O(1)−Ni(1)−O(2A)	99.2(1)
O(3A)−Ni(1)−O(2A)	83.0(1)	N(2)−Ni(1)−O(2A)	85.8(1)
O(1)−Ni(1)−N(1)	87.4(1)	O(3A)−Ni(1)−N(1)	90.5(1)
N(2)−Ni(1)−N(1)	89.7(1)	O(2A)−Ni(1)−N(1)	171.9(1)
O(1)−Ni(1)−O(1W)	85.8(1)	O(3A)−Ni(1)−O(1W)	93.3(1)
N(2)−Ni(1)−O(1W)	174.1(1)	O(2A)−Ni(1)−O(1W)	92.1(1)
N(1)−Ni(1)−O(1W)	93.0(1)		

[a] Symmetry code A: $1 - x, -y, 1 - z$. [b] Symmetry code A: $1 - x, y, -z + 1/2$.

$(L^1)(1\text{-methylimidazole})_2]_2$.[27] Each copper atom is coordinated by five donors to give a square pyramidal symmetry (C_{4v}) with the parameter[28] $\tau = 0$. The basal donors include therefore the pyridine nitrogen atom N(1), the water oxygen O(1W), the carboxylate oxygen O(1), and the carboxylate oxygen O(4A) [symmetry code A: $1 - x, -y, 1 - z$] from the other symmetric part of the dimmer, while the apical position is occupied by the DMF oxygen atom O(5). The Cu−O and Cu−N bond lengths are all within the range reported for square pyramidal environments (Table 4), and the Fe−C_{ring} distances are also in normal range.[24b,29]

Two kinds of classical O−H···O hydrogen bonds between the oxygen atoms of water molecules and the uncoordinated carboxyl oxygen atoms were found to stabilize the heterobimetallic box. The O(1W)···O(3) and O(1W)···O(2A) separations are 2.668(8) and 2.723(8) Å, while angles O(1W)−H(1WA)···O(3) and O(1W)−H(1WB)···O(2A) are 174 and 168°, respectively. The $\pi\cdots\pi$ stacking interactions were also found between the pyridine rings and the symmetric related ones which link the molecules one-by-one to form one-dimensional infinite chains (Figure 1b). The stacked pairs are parallel each other with the shortest interplanar atom···atom separation [C(13)···C(15B); symmetry code B, $2 - x, -y, 2 - z$] and the plane···plane separation between the stack pairs of ca. 3.62 and 3.57 Å, respectively, which are in agreement with results observed in the related stacked complexes.[30]

$Ni_2L^1{}_2(Py)_4(H_2O)$ (2). Figure 2a,b shows the molecular structure of the nickel complex **2**. The compound is best described as a double-stranded helix, and the two Ni(II) ions occupy the helical axis with the center-to-center separation of 3.56 Å. The water molecule occupies the special position $^1/_2$, y, $^1/_4$ and bridges the two nickel atoms. The complex possesses a crystallographic C_2 axis perpendicular to the helical Ni···Ni axis, and the four coplanar metals form a slightly distorted rhombus with the sides of 5.70 and 5.02 Å and the interior angles of 138 and 42°. Although the ligands cannot wrap around the two metal ions, chiral helices will result only when the two metal ions display the same absolute configurations.[31] It should be expected that the ligand used to build double helicates just needs to be able to transmit the chirality from one metal center to another. The octahedral geometric Ni(1) atom is ligated by two pyridines nitrogen atoms N(1) and N(2), one water molecule O(1W), and three oxygen atoms O(1), O(3A), and O(2A) [symmetry code A: $1 - x, y, 1/2 - z$] from three different carboxylic groups, respectively.

The ferrocenedicarboxylato moiety also exhibits a synperiplanar conformation (Chart 1) and acts as bridging ligand through carboxylato groups in a novel $\mu^2{:}\eta^2{:}\eta^1$-coordination mode: The oxygen atom O(2) is terminally bound to the related nickel atom Ni(1A), and the oxygen O(1) of the same carboxylic group is coordinated to nickel atom Ni(1) together with the third oxygen atom O(3). The torsion angle of disubstituted ferrocene is 0.9°, which is similar to that of the complex **1**, confirming the synperiplanar conformation of the ferrocene moiety. Classical O−H···O hydrogen bonds between the water molecule and the uncoordinated carboxyl oxygen atoms with the type O(1W)−H(1WA)···O(4A) were also found to stabilize this helical structure. The O(1W)···O(4A) separation is 2.595(6) Å, and the angle of O(1W)−H(1WA)···O(4A) is 158°.

(27) Zevaco, T. A.; Görls, H.; Dinjus, E. *Polyhedron* **1998**, *17*, 613.
(28) Addison, A. W.; Rao, T. N.; Reedijk, J.; van Rijn, J.; Verschoor, G. C. *J. Chem. Soc., Dalton Trans.* **1984**, 1349.
(29) Latif Abuhijleh, A.; Woods, C. *J. Chem. Soc., Dalton Trans.* **1992**, 1249.
(30) (a) Duan, C. Y.; Liu, Z. H.; You, X. Z.; Xue, F.; Mak, T. C. W. *Chem. Commun.* **1997**, 381. (b) He, C.; Duan, C. Y.; Fang, C. J.; Meng, Q. J. *J. Chem. Soc., Dalton Trans.* **2000**, 1207.
(31) (a) Albrecht, M.; Kotila, S. *Angew. Chem., Int. Ed. Engl.* **1995**, *34*, 2134. (b) Xu, J. D.; Parac, T. N.; Raymond, K. N. *Angew. Chem., Int. Ed. Engl.* **1999**, *38*, 2878. (c) Kersting, B.; Meyer, M.; Powers, R. E.; Raymond, K. N. *J. Am. Chem. Soc.* **1996**, *118*, 7221. (d) Serr, B. R.; Andersen, K. A.; Elliott, C. M.; Anderson, O. P. *Inorg. Chem.* **1988**, *27*, 4499.

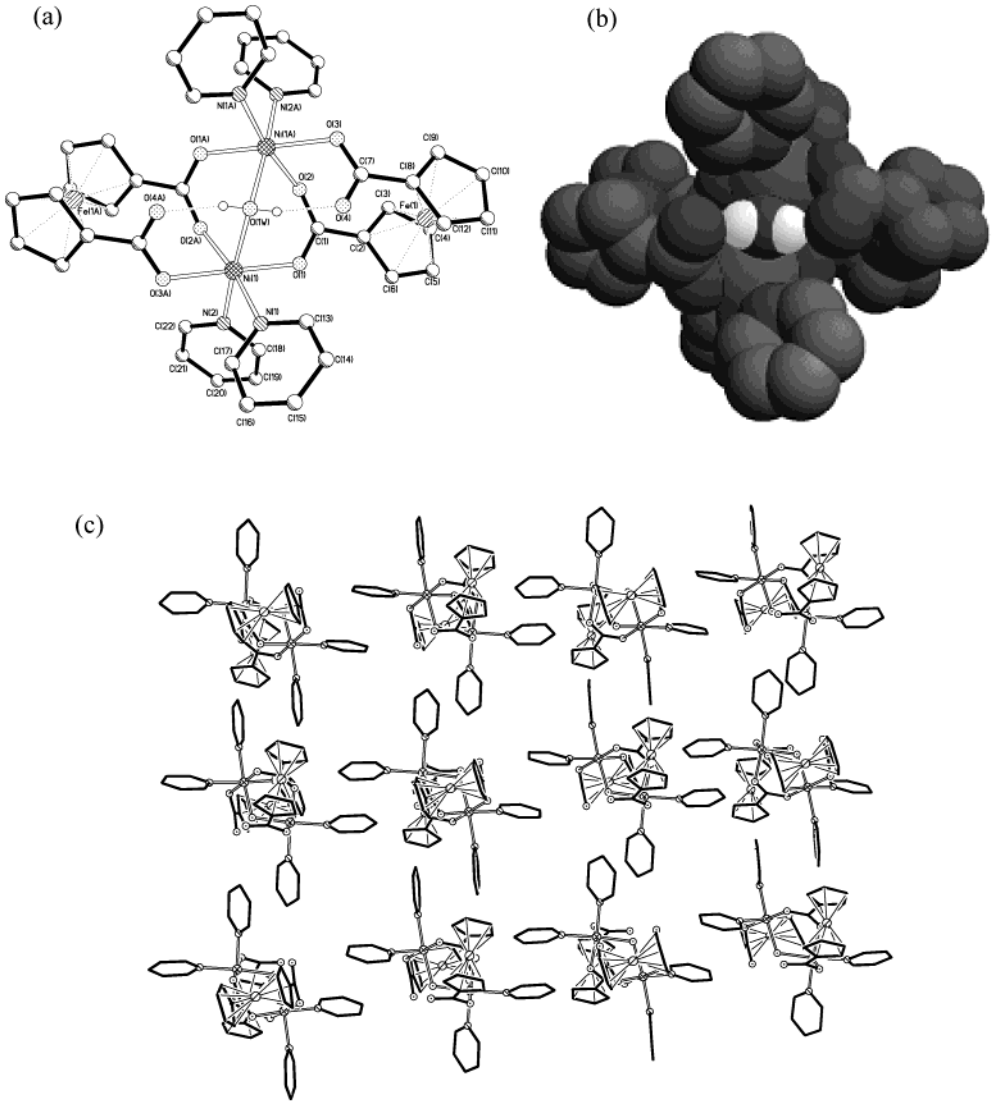

Figure 2. (a) Molecular structure of **2** with the atom numbering scheme. Hydrogen atoms apart from those on water molecules are omitted for clarity. (b) Spix drawing of **2**, which emphasizing the helical feature. (c) View of two-dimensional network in complex **2** showing intermolecular interactions in crystal packing.

The $\pi-\pi$ stacking interactions between the pyridine rings are found linking the molecules together to form a two-dimensional sheet (Figure 2c). The pyridine ring I [defined by the atoms N(1) and C(13)−C(17)] stacked to the symmetric related one IB [symmetry code B: $1 - x$, $1 - y$, $1 - z$] to give an one-dimensional chain with the plane-to-plane separation of ca. 3.42 Å and the shortest interplanar atom···atom [C(16)···C(14B)] separation of ca. 3.49 Å for the parallel stacked pairs. The chains are further aggregated to the two-dimensional state by the $\pi-\pi$ stacking interactions between pyridine ring II [defined by the atoms N(2) and C(18)−C(22)] and the symmetry-related one IIC (symmetry code C: $1 - x$, $-y$, $1 - z$) with the plane-to-plane separation of ca. 3.56 Å and the shortest interplanar atom···atom [C(18)···C(22C)] separation ca. 3.60 Å between the parallel stacking pairs. These distances are similar to the standard distance for a strong π-stacking interaction between two aryl rings.[32,33] At the same time, cooperative intermolecular C−H···π stacking interactions related to the Cp rings are also found in the crystal, which are characterized by the H(21A)···M [midpoint of the Cp ring C(2C)−C(6C)] distance of 2.99 Å and the C(21)···M distance of 3.86 Å, with a θ [C(21)−H(21A)···M] angle of 160°. It should be noted that such aromatic interaction is quite similar to the P4PE (parallel 4-fold phenyl embrace) motif described by Scudder and Dance[34] for tetraphenylphosphonium cations.

$[La_2L^1_3(CH_3OH)_4]_\infty$ (3). When the ligand H_2L^1 reacts with the d-block transition metal ions, the ligand L^1 tends to adopt cisoid conformations leading to the formation of the discrete molecular architectures. However, the stereochemical versatility and the high coordination numbers of the lanthanide metal ions may provide probability for constructing infinite networks. Crystal structure determination reveals the complex **3** as a two-dimensional network structure. Two types of coordination modes of ferrocenedicarboxylato(2−) ligands

(32) Shriver, D. F.; Arkins, P.; Langford, C. H. *Inorganic Chemistry*, 2nd ed.; W. H. Freeman and Co.: New York, 1997.
(33) Liu, Z. H.; Duan, C. Y.; Hu, J.; You, X. Z. *Inorg. Chem.* **1999**, *38*, 1719.
(34) (a) Scudder, M.; Dance, I. *J. Chem. Soc., Dalton Trans.* **1998**, 3167. (b) Scudder, M.; Dance, I. *J. Chem. Soc., Dalton Trans.* **1998**, 329.

with different conformations are present in this structure: (a) One ligand adopts a synperiplanar conformation with the torsion angle of ca. 7.4°. One of the two carboxylate groups [O(3) and O(4)] adopts a bidentate bridging mode connecting two different lanthanum atoms [La(1) and La(1A); symmetry code A, $2 - x$, $1 - y$, $2 - z$], whereas the other carboxylate group [O(1) and O(2)] adopts a bidentate chelating mode, chelating one lanthanum atom La(1) (Figure 3a), which is similar to that in the complex **2**. (b) In the other kind of ligand, the ferrocenedicarboxylato moiety shows an antiperiplanar conformation (Chart 1) with torsion angle of 180° (Figure 3b). Each carboxylate group adopts a bidentate μ^2:η^1:η^1-coordinative mode bridging two lanthanum atoms. Each lanthanum(III) atom is in an eight coordination geometry bound by the two oxygen atoms [O(5) and O(6D); symmetry code D, $1 - x$, $1 - y$, $2 - z$] from two carboxylate groups of two antiperiplanar ferrocenedicarboxylato(2−), four oxygen atoms [O(1), O(2), O(3), and O(4A)] from three different carboxylate groups of two synperiplanar ligands, and two oxygen atoms [O(7) and O(8)] from two methanol molecules, respectively. The shortest La···La distance is ca. 3.75 Å in the $La_2(syn\text{-}L^1)_2$ fragments, indicating the lack of the direct metal−metal interaction. The La−O bond lengths range from 2.403(5) to 2.601(4) Å (Table 5), similar to other related La−O distances.[6h] Each $La_2(syn\text{-}L^1)_2$ fragment is bridged by the carboxylate groups of the antiperiplanar ligands and connected through the antiperiplanar ferrocene moieties. The macrocyclic unit $[La_4(syn\text{-}L^1)_2(anti\text{-}L^1)_2]$ constitutes the basic building block of the structure. Every four La_4 building blocks are linked together through La−O bonding to induce a new small cycle, generating a two-dimensional layer structure with two kinds of pores (Figure 3b). Furthermore, adjacent layers are organized into 3-D network (Figure 3c) by the $\pi\cdots\pi$ stacking interactions between the Cp rings [defined by the atoms C(2)−C(6)] and the symmetry-related parallel one from adjacent layers with the shortest atom···atom separation of ca. 3.3 Å for C(3) and C(3E) [symmetry code E: $2 - x$, $1 - y$, $3 - z$].

$[Eu_2L^1_3(H_2O)_5]_\infty$ (4) and $[Gd_2L^1_3(CH_3OH)_2(H_2O)_3]_\infty$ (5). Crystal structural analysis shows that the complex **4** is also a 2-D coordination network constructed from the lanthanide−organometallic layers. Similar to **3**, all carboxyl groups are deprotonated with two types of coordination modes and conformations of ferrocenedicarboxylato ligands (Figure 4a), but differences from those in **3** are present: (a) Each carboxylate group of synclinal (eclipsed) ligands [O(1) and O(2)] adopts a bidentate chelating mode, chelating one europium atom Eu(1). (b) Each carboxylate group of antiperiplanar ligands (torsion angle 63.0°) adopts a less common tridentate μ^2:η^2:η^1-coordinating mode, in which one oxygen atom O(6) is terminally bound to the europium atom Eu(1) and the second oxygen O(5) is involved in a monatomic bridge between the two europium atoms Eu(1) and Eu(1A). The local coordination geometry around Eu(III) ion is nine-coordinate (Figure 4a). Two antiperiplanar ligands chelate to the atom Eu(1) through the carboxylate oxygen atoms [O(1)/O(2), O(3A)/O(4A); symmetry code A, $-x + 3/2$, y, $-z + 3/2$], occupying four coordination sites of Eu-

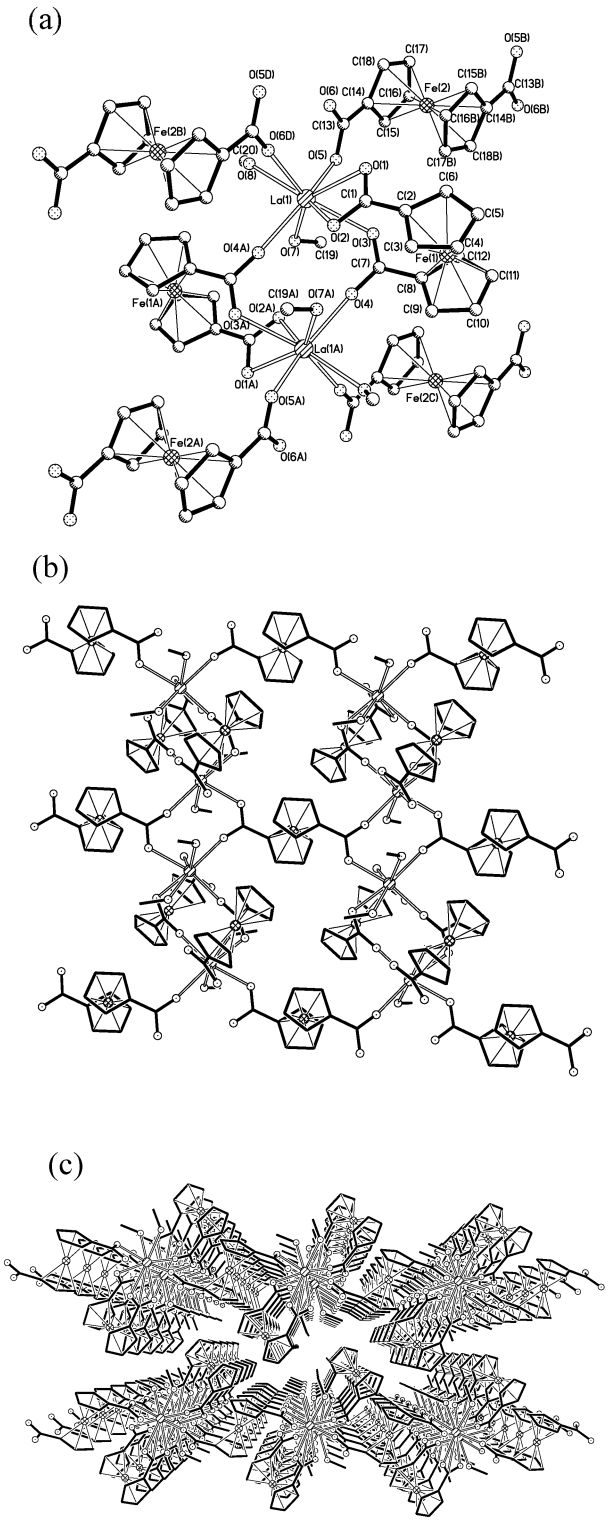

Figure 3. (a) View of **3** showing local coordination environment of La(III). Hydrogen atoms are omitted for clarity. (b) Two-dimensional layer of complex **3** showing the different conformations and coordination modes of the ligands. (c) Packing structure along the *a* axis.

(1). The remaining five coordination sites of Eu(1) are taken by three carboxylate oxygen atoms [O(5)/O(6), O(5B); symmetry code B, $1 - x$, $1 - y$, $1 - z$] from two antiperiplanar ligands and two oxygen atoms [O(1W) and O(2W)] from two coordinated water molecules. The nearest Eu···Eu distance is ca. 4.24 Å. Different from **3**, the

Table 5. Selected Bond Lengths (Å) and Bond Angles (deg) of Compounds **3**−**5** with Estimated Standard Deviations in Parentheses

3[a]

La(1)−O(4A)	2.403(5)	La(1)−O(5)	2.443(5)	La(1)−O(7)	2.561(4)	La(1)−O(2)	2.590(4)
La(1)−O(6D)	2.456(4)	La(1)−O(3)	2.535(4)	La(1)−O(1)	2.601(4)	La(1)−O(8)	2.594(4)
O(4A)−La(1)−O(5)	144.4(2)	O(4A)−La(1)−O(6D)	91.0(2)	O(4A)−La(1)−O(2)	78.7(1)	O(5)−La(1)−O(2)	133.3(1)
O(5D)−La(1)− O(6)	107.5(2)	O(4A)−La(1)−O(3)	105.4(2)	O(6D)−La(1)−O(2)	80.5(1)	O(3)−La(1)−O(2)	73.5(1)
O(5)−La(1)−O(3)	76.4(2)	O(6D)−La(1)−O(3)	145.4(1)	O(5)−La(1)−O(1)	85.7(2)	O(4A)−La(1)−O(1)	128.7(1)
O(3)−La(1)−O(1)	68.7(1)	O(6D)−La(1)−O(1)	77.3(1)				

4[b]

Eu(1)−O(5B)	2.360(5)	Eu(1)−O(6)	2.410(6)	Eu(1)−O(5)	2.880(5)	Eu(1)−O(1W)	2.458(5)
Eu(1)−O(3A)	2.414(5)	Eu(1)−O(1)	2.441(4)	Eu(1)−O(4A)	2.463(5)	Eu(1)−O(2)	2.495(5)
O(5B)−Eu(1)−O(6)	120.6(2)	O(5B)−Eu(1)−O(3A)	98.4(2)	O(1)−Eu(1)−O(4A)	125.4(2)	O(5B)−Eu(1)−O(2)	128.1(2)
O(6)−Eu(1)−O(3A)	138.4(2)	O(5B)−Eu(1)−O(1)	76.0(2)	O(6)−Eu(1)−O(2)	73.0(2)	O(3A)−Eu(1)−O(2)	71.6(2)
O(6)−Eu(1)−O(1)	94.3(2)	O(3A)−Eu(1)−O(1)	80.8(2)	O(5B)−Eu(1)−O(5)	72.5(2)	O(4A)−Eu(1)−O(2)	122.5(2)
O(6)−Eu(1)−O(4A)	139.4(2)	O(5B)−Eu(1)−O(4A)	81.3(2)	O(3A)−Eu(1)−O(5)	156.4(2)	O(1)−Eu(1)−O(5)	75.9(1)
O(4A)−Eu(1)−O(5)	140.9(1)	O(2)−Eu(1)−O(5)	96.5(2)				

5[c]

Gd(1)−O(6)	2.345(5)	Gd(1)−O(5B)	2.370(5)	Gd(1)−O(1)	2.427(4)	Gd(1)−O(6B)	2.943(5)
Gd(1)−O(3A)	2.402(5)	Gd(1)−O(7)	2.403(5)	Gd(1)−O(4A)	2.475(5)	Gd(1)−O(2)	2.502(4)
O(6)−Gd(1)−O(5B)	118.2(2)	O(6)−Gd(1)−O(3A)	98.3(2)	O(6)−Gd(1)−O(2)	127.9(2)	O(4A)−Gd(1) −O(2)	122.8(2)
O(5B)−Gd(1)−O(3A)	140.2(2)	O(5B)−Gd(1)−O(1)	92.0(2)	O(3A)−Gd(1)−O(2)	71.7(2)	O(2)−Gd(1)−O(6B)	96.9(1)
O(6)−Gd(1)−O(1)	75.8(2)	O(6)−Gd(1)−O(4A)	81.2(2)	O(6)−Gd(1)−O(6B)	71.4(2)	O(1)−Gd(1)−O(6B)	74.7(1)
O(3A)−Gd(1)−O(1)	81.6(2)	O(5B)−Gd(1)−O(4A)	141.5(2)	O(3A)−Gd(1)−O(6B)	155.8(2)	O(4A)−Gd(1)−O(6B)	140.3(1)
O(1)−Gd(1)−O(4A)	126.0(2)	O(5B)−Gd(1)−O(2)	73.4(2)				

[a] Symmetry code: A, $2 - x$, $1 - y$, $2 - z$; D, $1 - x$, $1 - y$, $2 - z$. [b] Symmetry code: A, $-x + 3/2$, y, $-z + 3/2$; B, $1 - x$, $1 - y$, $1 - z$. [c] Symmetry code: A, $-x + 1/2$, y, $-z + 1/2$; B, $-x$, $1 - y$, $-z$.

macrocyclic unit constituted the basic building block of the structure is $[Eu_6(syn\text{-}L^1)_2(anti\text{-}L^1)_2]$. Every Eu_6 building unit is linked together through the Eu−O bonding, creating a two-dimensional brick well structure with two kinds of pores (Figure 4b). Adjacent layers are organized into a 3-D network by very strong $\pi\cdots\pi$ stacking interactions between the Cp ring I [defined by the atoms C(2)−C(6)] and the parallel symmetric one ID [symmetry code D: $2 - x$, $-1 - y$, $1 - z$] from the adjacent layers in an offset fashion with a face-to-face distance of 3.23 Å, creating shuttle-shaped channels with an effective size of ca. 3×8 Å[35] as shown in Figure 4c. The lattice water molecules are clathrated in these channels.

The complex **5** is isostructural with **4** expect that one of the coordinated water molecules is instead replaced by one methanol molecule (Figure 5).

$Ln_2L^2_6(CH_3OH)_2(H_2O)_5$ [Ln = La (6), Eu (7), and Gd (8)]. The compounds **6**−**8** are all isostructural. The molecular structure of **6** is shown in Figure 6a as a representative. Obviously, the molecular entity is binuclear and possesses an inversion center. Of the six ferrocenecarboxylato anions, two act as bridging ligands through their carboxylato groups in the less common μ^2:η^2:η^1-fashion. In this case one oxygen atom [O(2), O(2A)] is terminally coordinated to the related lanthanum ions [La(1), La(1A)] and the second oxygen atom [O(1), O(1A)] is involved in a monatomic bridge between the two lanthanide ions (Table 6). Each of the four remaining anions chelates a metal ion [La(1), La(1A)]. As a result of the inversion center, the La(1)−O(1)−O(1A)−La(1A) double bridging network is perfectly planar. Furthermore, the coordination of each lanthanide ions is completed to nine by two water molecules.

Interestingly, these windmill-shaped molecules are stacked through the C−H$\cdots\pi$ interactions between the Cp rings expanding to a 2-D network structure (Figure 6b). The distance between the atom C(8) and the centroid (M) of the Cp ring [defined by the atoms C(18B)−C(22B); symmetry code B, x, $-1 + y$, $-1 + z$] is 3.64 Å (H$\cdots$M, 2.83 Å; C−H$\cdots$M, 142°). The separation between the atom C(21) and the centroid of the Cp ring [defined by the atoms C(29C)−C(33C); symmetry code C, $1 - x$, $1 - y$, $1 - z$] is 3.67 Å [H$\cdots$M, 3.01 Å; C−H$\cdots$M, 127°]. It should be noted that these distances are shorter than those found in the crystal structure of benzene (3.78 Å)[36] and only very few results related to the C−H$\cdots\pi$ interactions between ferrocene moieties of metal complex molecules had been reported in the literature.

Redox Properties of Compounds 1−8. The differential pulse voltammetry (DPV) technique is usually employed to obtain well-resolved potential information, while the individual redox processes for the multinuclear complexes are poorly resolved in the CV experiment, in which individual $E_{1/2}$ potentials cannot be easily or accurately extracted from these data.[37]

The solution-state differential pulse voltammetries of the complexes **1** and **2** (Figure 7) show two peaks with half-wave potentials ($E_{1/2}$) at 0.62 and 0.77 V for **1** and 0.45 and 0.71 V for **2**, respectively, corresponding to the two single-

(35) The channel dimensions are estimated from the van der Waals radii for carbon (1.70 Å) and oxygen (1.40 Å).

(36) Bacon, G. E.; Curry, N. A.; Wilson, S. A. *Proc. R. Soc. London, Ser. A* **1964**, *279*, 98.

(37) (a) Serr, B. R.; Andersen, K. A.; Elliott, C. M.; Anderson, O. P. *Inorg. Chem.* **1988**, *27*, 4499. (b) Richardson, D. E.; Taube, H. *Inorg. Chem.* **1981**, *20*, 1278.

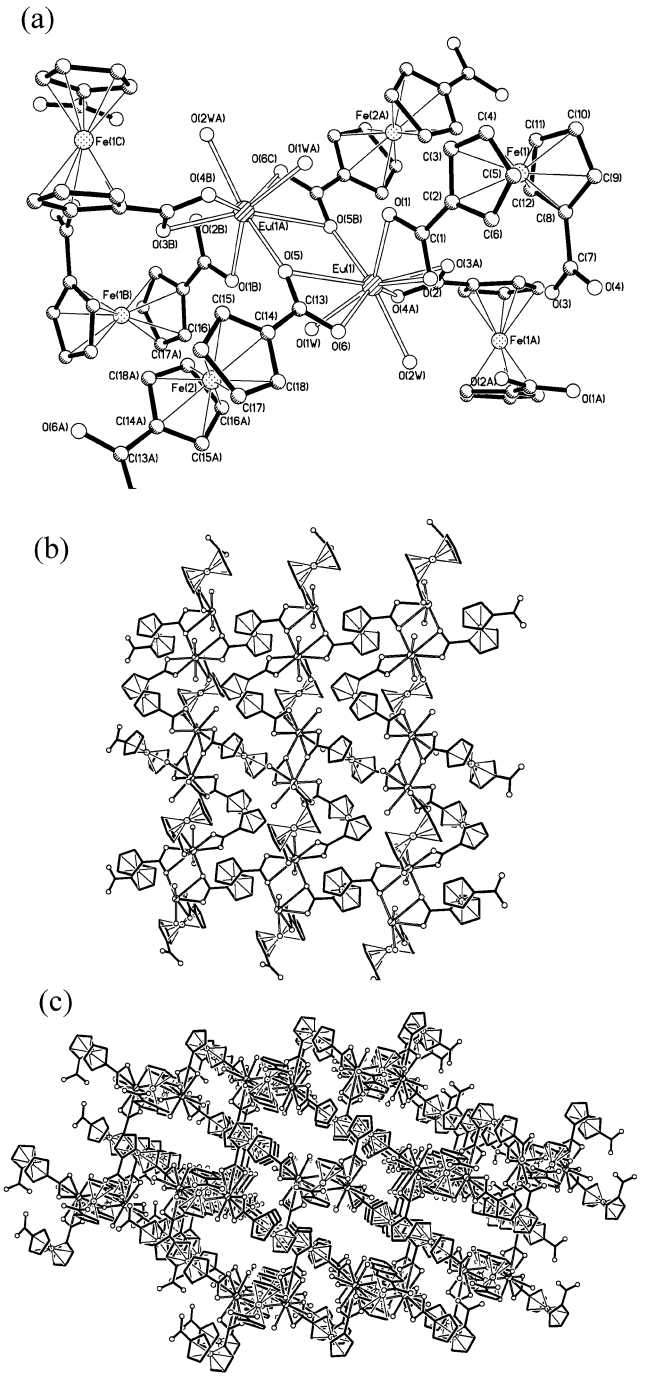

Figure 4. (a) View of **4** showing the local coordination environment of Eu(III). Hydrogen atoms and solvent molecules of crystallization are omitted for clarity. (b) Two-dimensional layer of complex **4** showing the different conformations and coordination modes of the ligands. (c) Perspective view showing the 3-D network along the *b* axis in **4**. The lattice water molecules are omitted for clarity.

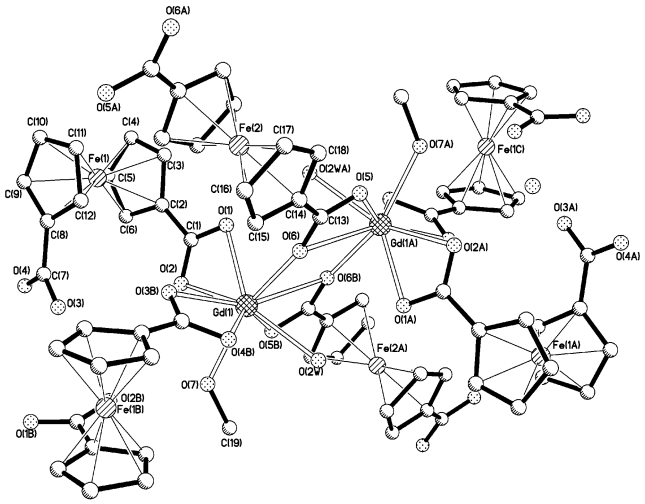

Figure 5. View of **5** showing the local coordination environment of Gd(III). Hydrogen atoms and solvent molecules of crystallization are omitted for clarity.

electron oxidations of the ferrocenyl moieties. The ΔE values of ca. 0.15 and 0.26 V indicate strong interactions between two ferrocene moieties in the corresponding complexes.

In general, the molecules containing metallocene units could accommodate a particular metal ion at its coordination site and undergo a concurrent redox change.[38] And polyferrocenes generally undergo reversible one-electron oxidations, with the number of waves being determined by the number of ferrocenyl units. The half-wave potentials of the redox processes and the separation (ΔE) between consecutive waves vary over a wide range depending on the nature of the compounds. It is postulated that ΔE mainly depends on a number of factors:[39] (1) Major structural changes such as bond making and breaking, changes in coordination number, and severe changes in coordination geometry upon charge transfer can shift the comproportionment equilibrium. (2) If the metal ions are in a close proximity, a through-space Coulomb interaction may be important. An n^+ ion will be more readily reduced than an $(n - 1)^+$ ion on the basis of electrostatic consideration alone, which will increase ΔE. (3) Electronic delocalization in mixed oxidation states will enhance the stability of these species with resulting increases in ΔE.

The tetranuclear complexes **1** and **2** were designed to help quantitatively define some of these effects. (1) Although the bridged metal moieties can accommodate a range of coordination geometry, it is likely that only negligible structural changes accompany one-electron oxidation of these complexes, since crystallographic data on ferrocene[40] and its salts[41] indicate that the oxidation state and charge of the iron atom have almost no effect on the interatomic distances. (2) The through-space metal−metal Coulomb contribution to the Fe(II)/Fe(III) oxidation potential in the Fc−M−Fc complexes is essentially constant and could be cancelable, since the distances between iron atoms are almost same for the two metal-bridged biferrocene complexes (10.3 Å for **1** and 10.0 Å for **2**), which are much larger than 7.6 Å, the average

(38) Beer, P. D. *Adv. Inorg. Chem.* **1992**, *39*, 79.

(39) (a) Creutz, C.; Taube, H. *J. Am. Chem. Soc.* **1973**, *95*, 1086. (b) Callahan, R. W.; Keene, F. R.; Mayer, T. J.; Salmon, D. J. *J. Am. Chem. Soc.* **1974**, *96*, 7827. (c) Weaver, T. R.; Mayer, T. J.; Adeylmi, S. A.; Brown, G. M.; Eckberg, R. P.; Hatfield, E.; Johnson, E. C.; Murray, R. W.; Unterker, D. *J. Am. Chem. Soc.* **1975**, *97*, 3039. (d) Morrison, W. H., Jr.; Krogsrud, S.; Hendrickson, D. N. *Inorg. Chem.* **1973**, *12*, 1998.

(40) Rosenblum, M. *Chemistry of the Iron Group Metallocenes*; New York, 1965.

(41) Berstern, T.; Herbstein, F. H. *Acta Crystallogr., Sect B* **1968**, *24*, 1546.

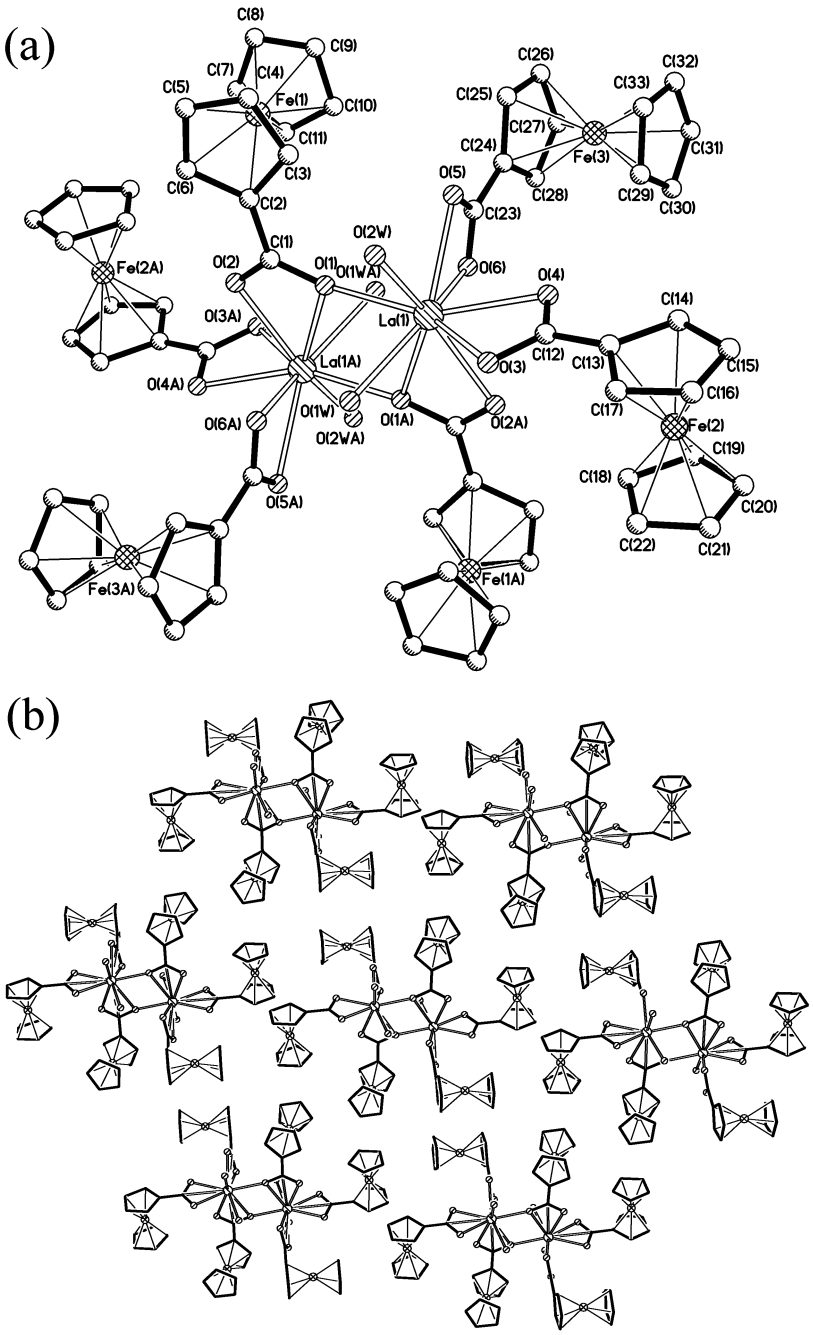

Figure 6. (a) Molecular structure of **6** with the atom numbering scheme. Hydrogen atoms and solvent molecules of crystallization are omitted for clarity. (b) View of the two-dimensional network in complex **6** showing intermolecular interactions in crystal packing.

encounter diameter between the ferrocene and ferrocenium ion in solution. In fact, these metal-bridged biferrocene complexes designed here are used to minimize the through-space iron−iron interaction between the ferrocenyl moieties. Such an electrochemical communication behavior might be explained semiquantitatively on the basis of through-bond interaction. (3) The different electrochemistries of the complexes **1** and **2** should contribute to the different coordination geometries of the bridged metal moieties. The crystal structure analyses of complexes **1** and **2** show a major structural difference which might influence the through-bond interaction: (a) In complex **1**, the two ferrocenyl moieties were bridged by four O−metal linkers, while, in complex **2**, six O−metal linkers were found to bridge the two ferrocene moieties, which might enhance the through-bond interation between them. (b) The Ni···Ni separation in **2** (3.6 Å), much shorter than the Cu···Cu separation in **1** (4.9 Å), as well as the Ni−O(W)−Ni bridge is suggested to favor the electronic delocalization among the whole molecule of complex **2**.

In comparison, the solid-state differential pulse voltammetries of the compounds **3**−**5** are investigated and show broad single peaks at 0.40, 0.31, and 0.32 V (vs Ag/AgCl), respectively, which is probably due to the different conformations and coordination modes of ferrocene moieties in the solid state. The solution-state differential pulse voltammetric

Table 6. Selected Bond Lengths (Å) and Bond Angles (deg) of Compounds **6**−**8** with Estimated Standard Deviations in Parentheses

			6[a]				
La(1)−O(2A)	2.464(3)	La(1)−O(1)	2.472(3)	La(1)−O(4)	2.516(3)	La(1)−O(1A)	2.680(3)
La(1)−O(6)	2.484(3)	La(1)−O(1W)	2.495(3)	La(1)−O(5)	2.538(3)	La(1)−O(3)	2.574(3)
O(2A)−La(1)−O(1)	120.1(1)	O(2A)−La(1)−O(6)	79.7(1)	O(2A)−La(1)−O(3)	78.0(1)	O(5)−La(1)−O(3)	114.1(1)
O(1)−La(1)−O(6)	78.9(1)	O(1)−La(1)−O(4)	155.6(1)	O(6)−La(1)−O(3)	134.6(1)	O(1)−La(1)−O(1A)	70.3(1)
O(2A)−La(1)−O(4)	74.2(1)	O(2A)−La(1)−O(5)	123.3(1)	O(6)−La(1)−O(1A)	74.8(1)	O(5)−La(1)−O(1A)	123.3(1)
O(6)−La(1)−O(4)	85.0(1)	O(1)−La(1)−O(5)	81.3(1)	O(4)−La(1)−O(1A)	122.9(1)	O(3)−La(1)−O(1A)	116.8(1)
O(4)−La(1)−O(5)	74.3(1)	O(1)−La(1)−O(3)	146.2(1)				
			7[b]				
Eu(1)−O(2A)	2.379(3)	Eu(1)−O(1)	2.389(3)	Eu(1)−O(1A)	2.628(3)	Eu(1)−O(4)	2.429(3)
Eu(1)−O(6)	2.409(3)	Eu(1)−O(1W)	2.415(3)	Eu(1)−O(5)	2.461(3)	Eu(1)−O(3)	2.519(3)
O(2A)−Eu(1)−O(1)	120.4(1)	O(2A)−Eu(1)−O(6)	79.6(1)	O(1)−Eu(1)−O(3)	146.6(1)	O(6)−Eu(1)−O(3)	133.6(1)
O(1)−Eu(1)−O(6)	79.7(1)	O(1)−Eu(1)−O(4)	153.9(1)	O(5)−Eu(1)−O(3)	114.3(1)	O(4)−Eu(1)−O(1A)	124.6(1)
O(2A)−Eu(1)−O(4)	74.9(1)	O(2A)−Eu(1)−O(5)	125.6(1)	O(1)−Eu(1)−O(1A)	69.2(1)	O(3)−Eu(1)−O(1A)	116.9(1)
O(6)−Eu(1)−O(4)	83.1(1)	O(1)−Eu(1)−O(5)	80.5(1)	O(6)−Eu(1)−O(1A)	75.0(1)	O(5)−Eu(1)−O(1A)	124.1(1)
O(4)−Eu(1)−O(5)	73.5(1)	O(2A)−Eu(1)−O(3)	76.7(1)				
			8[c]				
Gd(1)−O(2A)	2.366(3)	Gd(1)−O(1)	2.366(3)	Gd(1)−O(1A)	2.634(3)	Gd(1)−O(4)	2.414(3)
Gd(1)−O(1W)	2.390(3)	Gd(1)−O(6)	2.392(3)	Gd(1)−O(5)	2.443(3)	Gd(1)−O(3)	2.502(3)
O(2A)−Gd(1)−O(1)	120.2(1)	O(2A)−Gd(1)−O(6)	79.6(1)	O(1)−Gd(1)−O(3)	146.5(1)	O(5)−Gd(1)−O(3)	114.7(1)
O(1)−Gd(1)−O(6)	79.8(1)	O(1)−Gd(1)−O(4)	153.7(1)	O(6)−Gd(1)−O(3)	133.6(1)	O(1)−Gd(1)−O(1A)	69.0(1)
O(2A)−Gd(1)−O(4)	75.2(1)	O(6)−Gd(1)−O(4)	82.8(1)	O(5)−Gd(1)−O(1A)	123.7(1)	O(6)−Gd(1)−O(1A)	74.7(1)
O(1)−Gd(1)−O(5)	80.2(1)	O(2A)−Gd(1)−O(5)	125.9(1)	O(3)−Gd(1)−O(1A)	117.0(1)	O(4)−Gd(1)−O(1A)	124.7(1)
O(4)−Gd(1)−O(5)	73.7(1)	O(2A)−Gd(1)−O(3)	76.8(1)				

[a] Symmetry code A: $1 - x, 1 - y, 1 - z$. [b] Symmetry code A: $1 - x, 1 - y, 1 - z$. [c] Symmetry code A: $1 - x, 1 - y, 1 - z$.

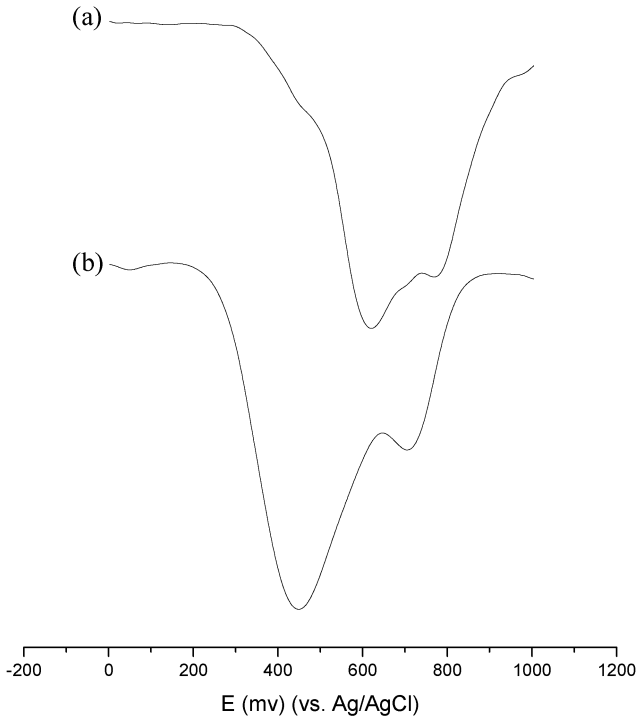

Figure 7. Differential pulse voltammogram of complexes **1** (a) and **2** (b) ($\sim 1.0 \times 10^{-3}$ M) in DMF containing *n*-Bu_4NClO_4 (0.1 M) at a scanning rate of 20 mV s^{-1} (vs Ag/AgCl).

studies on compounds **6**−**8** all show single peaks at 0.53, 0.56, and 0.55 V (vs Ag/AgCl), respectively, which suggests that all six ferrocene units in each compound are oxidized at the same potential. In these lanthanide−ferrocenyl compounds, it seems that the interations between the ferrocenyl moieties might be held back by the bridged lanthanide ions.

Conclusion

We have shown that the reaction of ferrocene-based bridging ligands with metal ions leads to the formation of a series of redox-active coordination polymers. The conformational flexibility of the ligand may lead to various assembled structures. The incorporation of the ferrocene moiety into the metal−organic frameworks leads to unprecedented and different topological structures that are of importance not only for their aesthetic appeal but also for their potential use in the design of functional solids.

Acknowledgment. This work was supported by the National Natural Science Foundation of China. We thank Dr. He Cheng of Peking University and Mr. Liu Yong-jiang of Nanjing University for collecting the crystal data.

Supporting Information Available: Tables of detailed crystallographic data, atomic positional parameters, anisotropic displacement parameters, and bond length and angles in CIF format. This material is available free of charge via the Internet at http://pubs.acs.org.

IC0205132